Catalysis Today 151 (2010) 8–13

Contents lists available at ScienceDirect

Catalysis Today

journal homepage: www.elsevier.com/locate/cattod

Synthesis and characterization of nitrogen-doped TiO_2/AC composite for the adsorption–photocatalytic degradation of aqueous bisphenol-A using solar light

Pow-Seng Yap [a], Teik-Thye Lim [a,*], Melvin Lim [a], Madhavi Srinivasan [b]

[a] School of Civil and Environmental Engineering, Nanyang Technological University, 50 Nanyang Avenue, Singapore 639798, Singapore
[b] School of Materials Science and Engineering, Nanyang Technological University, 50 Nanyang Avenue, Singapore 639798, Singapore

ARTICLE INFO

Article history:
Available online 7 February 2010

Keywords:
Titanium dioxide
Activated carbon
Photocatalysis
Bisphenol-A
Solar energy

ABSTRACT

A photocatalytic composite, namely nitrogen-doped titanium dioxide supported on activated carbon, or N-TiO_2/AC, was synthesized using the sol–gel method. This composite was characterized using X-ray diffraction (XRD), N_2 adsorption–desorption isotherm, UV–vis spectrophotometry, X-ray photoelectron spectroscopy (XPS) and transmission electron microscopy (TEM). The titania was found to consist predominantly of anatase. The AC-supported N-TiO_2 had a smaller average crystallite size (ca. 5.0 nm) as compared to the unsupported N-TiO_2 (ca. 5.4 nm). XPS revealed that interstitial nitrogen doping occurred in N-TiO_2 and N-TiO_2/AC. Observations under TEM revealed that N-TiO_2 nanocrystals were anchored on the surface of the AC. The dual-functionality properties of N-TiO_2/AC were evaluated using bisphenol-A (BPA) as the target pollutant in the aqueous phase. The effect of pH and influence of excitation wavelengths were investigated. Inhibition of BPA adsorption occurred at pH 11.0, thus resulted in slower kinetics of BPA photodegradation. N-TiO_2/AC was found to be photoresponsive under visible-light (420–630 nm) illumination.

1. Introduction

Among various advanced oxidation processes (AOPs), heterogeneous photocatalysis appears to be an appealing option for water and wastewater treatment, because it (i) does not require the usage of toxic, hazardous, and expensive chemicals, (ii) allows the destruction of a myriad of organic aqueous pollutants including recalcitrant compounds, and (iii) is more energy efficient compared to sonolysis and photolysis. Titanium dioxide (TiO_2) stands out to be a promising photocatalyst because it is chemically and biologically stable, available at competitive costs, has low toxicity, and typically yields high photocatalytic effect under UV irradiation [1].

To overcome mass transfer limitation associated with TiO_2 application in water treatment, the slurry system in which TiO_2 powder is well dispersed in suspension is favourable over the fixed system. For the slurry system, the nanosized TiO_2 particles can be mounted to suitable particulate support to enhance its separation from the treated water, and to increase adsorption of target pollutant to the supported TiO_2. Activated carbon (AC) emerges as one of the most attractive TiO_2 support [2]. The favourable characteristics of AC include: (1) it has strong affinity for a wide range of organic pollutants, (2) it has a long tradition of proven application for water and wastewater treatment, (3) it can be conveniently obtained at competitive cost and available in a variety of particle sizes, and (4) in contact with TiO_2, it has the capability to extend the separation lifetime of photogenerated e^-/h^+ [3] and thus increasing the quantum efficiency of TiO_2.

Meanwhile, various modifications of TiO_2 to render it photoactive under visible-light have also been attempted. Some notable techniques include the modification with noble metals [4,5], metal-ions [6–8] or anions [9–11]. Considering the thermal instability of metal-ions [12] and expensive costs of noble metals, anion doping appears as the more favourable method. Among the possible anions, nitrogen is an attractive dopant for TiO_2 as findings have shown that N-TiO_2 induces desirable visible-light photoresponsive properties [13,14].

In recent years, bisphenol-A (BPA) has attracted increasing public concern, after it was found to leach out from polycarbonate baby bottles [15]. Albeit useful as a chemical for the production of polycarbonate bottles, epoxy resins, flame retardants, etc. [16], BPA has been reported to cause adverse environmental and health effects because it is an endocrine disrupting compound (EDC) that poses potential estrogenic and toxicological risk [17–19]. Of late, numerous occurrences of BPA in our natural and engineered water systems have been reported worldwide [20–23]. Hence, it is necessary to develop the economically viable and sustainable treatment technologies to tackle this issue.

The current project embarks on developing a dual-functional composite, namely nitrogen-doped TiO_2 supported on activated carbon (N-TiO_2/AC). In this study, N-TiO_2/AC was prepared and

* Corresponding author. Tel.: +65 6790 6933; fax: +65 6791 0676.
E-mail address: cttlim@ntu.edu.sg (T.-T. Lim).

0920-5861/$ – see front matter © 2010 Elsevier B.V. All rights reserved.
doi:10.1016/j.cattod.2010.01.012

deployed to remove BPA in the aqueous system. Specifically, the effect of solution pH and influence of excitation wavelengths were examined.

2. Experimental

2.1. Synthesis of N-TiO_2/AC composite

N-TiO_2/AC was synthesized using the sol–gel method. Ultrapure water (18.2 MΩ cm) was used for preparing all aqueous solutions. Powdered AC (Norit SA UF, Switzerland) was purchased from Behn Meyer, Singapore. The powdered AC was first rinsed with ultrapure water, pre-treated in NaOH solution, and finally vacuum-dried. Titanium tetraisopropoxide (TTIP) (Merck) was used as the Ti-precursor, while the nitrogen source was urea (Merck). Absolute ethanol was used as a solvent. HCl was used to acidify absolute ethanol, and this solution was mixed with a separate solution comprising absolute ethanol and TTIP. Urea solution was added dropwise and the resulting solution was left to mix overnight. Subsequently, ultrapure water was added for hydrolysis. This was followed by the immersion of powdered AC and the slurry suspension was stirred to ensure uniform dispersion. After that, the solution was gradually heated, and the gel-coated AC precipitates were recovered and vacuum-dried. For comparison, N-TiO_2 powder was prepared without addition of AC, while TiO_2 powder was prepared without addition of urea and AC. Finally, these vacuum-dried samples were calcined using a tube furnace at 400 °C for 2 h under N_2 gas flow, to yield the N-TiO_2/AC, N-TiO_2 and TiO_2, respectively.

2.2. Characterization of N-TiO_2/AC composite

The crystallinity of N-TiO_2/AC, N-TiO_2 and TiO_2 was examined using a X-ray diffractometer (Bruker AXS D8 Advance) with Cu Kα radiation of λ = 1.54 Å, at the condition of 40 kV and 40 mA. Porosimetric studies were carried out using nitrogen adsorption–desorption at 77 K (QuantaChrome Autosorb-1 Analyzer) to obtain the Brunauer–Emmett–Teller (BET) surface areas (S_{BET}) and Barrett-Joyner-Halenda (BJH) pore size distributions of the materials. The surface chemistry of samples was probed using X-ray photoelectron spectroscopy (XPS) (KratosAXIS Ultra spectrometer), operated with monochromatic Al Kα X-rays (1486.71 eV). Calibration of binding energies for all elements in XPS spectra was made with reference to adventitious carbon (C1s = 284.8 eV). Photoactivity of selected materials was studied with a UV–vis spectrophotometer (Lambda 35, PerkinElmer), equipped with an integrating sphere accessory. The morphology of N-TiO_2/AC and surface N-TiO_2 wt% were studied using a scanning electron microscope (SEM)–energy dispersive X-ray (EDX) (JSM-6360 microscope with JED-2300 X-ray analyzer). Bulk N-TiO_2 wt% was determined using gravimetry method, i.e. ashing in a muffle furnace (Nabertherm) at 700 °C for 2 h. The N-TiO_2 crystal perfections and the interfacial titania coatings on AC were probed using the transmission electron microscope (TEM) (JEOL 2010F microscope).

2.3. Analysis of BPA

2.3.1. BPA chemical

BPA was purchased from Merck, and was used without any pretreatment. All BPA solutions were prepared with ultrapure water (18.2 MΩ cm).

2.3.2. Adsorption experiment

Kinetic studies on the adsorption of BPA by N-TiO_2/AC and virgin AC were carried out in the dark and it was found that adsorption equilibrium was achieved within 1.5 h (data not shown). Thus, 1.5 h was chosen as the adsorption equilibrium time. Batch equilibrium adsorption experiments were conducted in the dark over a range of initial concentrations to obtain the adsorption isotherm of BPA on N-TiO_2/AC and virgin AC, respectively. The solution pH were measured with a pH meter (Horiba, Japan) and the pH was adjusted using either HCl (1.0 M) or NaOH (1.0 M) solutions. After adsorption equilibrium, the final pH of BPA solutions was measured. Finally, aliquots were sampled and filtered using a 0.45 μm cellulose acetate membrane syringe filter. High-performance liquid chromatography (HPLC) (PerkinElmer) was used to analyze the BPA concentrations. The mobile phase used was ultrapure water/acetonitrile (20:80, v/v), with a flow rate of 1.0 mL/min through a C18 column (Inertsil ODS-3, 4.6 mm i.d. × 150 mm length, 5 μm). The detection wavelength was 225 nm and a temperature of 25 °C was maintained for the column throughout analysis.

2.3.3. Photocatalytic degradation (PCD) experiment

Prior to all PCD experiments, adsorption of BPA in the dark was performed to allow for adsorption equilibrium. PCD experimental runs were carried out using a solar simulator (Newport, USA), equipped with a Xenon arc lamp of 150 W. The light intensity of the solar spectrum was measured to be ca. 1000 W/m^2 (as measured with a digital power meter, EDTM). The UV and visible-light intensity were found to constitute ca. 6.5% and 40%, respectively, of the light intensity for solar spectrum. The initial concentration of BPA solution used was 36 mg/L and the BPA solution volume was 250 mL. Dosage of N-TiO_2/AC used was 0.25 g/L. PCD experiments were conducted without aeration and a quartz cover was placed on top of the glass reactor to minimize loss of water due to evaporation. The passage of electromagnetic waves with specific ranges of wavelengths (i.e. 280–400 nm and 420–630 nm) was controlled using dichroic mirrors. An additional polycarbonate filter was included for the case of visible-light (420–630 nm) experiments in order to reduce the UV to less than 10 μW/cm^2 (as measured with AccuMAX XRP-3000 radiometer). PCD studies on BPA were also conducted using TiO_2, N-TiO_2 and Degussa P25 (all of which with the comparable photocatalyst loading) at the same excitation wavelengths as that of the experiments with N-TiO_2/AC composite.

3. Results and discussion

3.1. Characteristics of N-TiO_2/AC composite

The physical properties of the 30 wt% N-TiO_2/AC composite, along with that of various materials, are shown in Table 1. The higher surface N-TiO_2 wt% of N-TiO_2/AC composite as compared to its bulk wt% was because SEM microscope only analyzed the elemental composition on the surface of the composite. The reduction of S_{BET} for N-TiO_2/AC composite as compared to that of virgin AC was attributed to the deposition of N-TiO_2 on AC surface. Coatings of N-TiO_2 on AC were also investigated using EDX and further examinations under the SEM confirmed that the titania was supported with good integrity on the AC surfaces (data not shown).

The mineralogical properties of N-TiO_2/AC composite are as shown in the XRD pattern (Fig. 1). The crystal phases of N-TiO_2 and TiO_2 consisted of predominantly anatase. Crystallite sizes were estimated using the Debye–Scherrer's equation [24]. TiO_2 crystals (ca. 5.7 nm) were relatively larger than N-TiO_2 crystals (ca. 5.4 nm). This indicates that nitrogen-doping had relatively restricted the growth of the TiO_2 crystals. N-TiO_2 nanocrystals supported on AC (ca. 5.0 nm) were smaller than unsupported N-TiO_2. This is due to the anti-calcination effect, whereby the production of interfacial energy between the surface of AC and the N-TiO_2 particles prevented the agglomeration of N-TiO_2 on AC [25].

Table 1
Physical characteristics for various materials.

Samples	S_{BET} (m^2/g)	BJH predominant pore size (nm)	BJH cumulative desorption pore volume (cm^3/g)	Bulk wt% of N-TiO_2[a]	Surface wt% of N-TiO_2[b]	At% of N[c]	Mass% of N[c]
Virgin AC	799	1.4	0.39	–	–	–	–
P25	57.8	2.3	0.14	–	–	–	–
TiO_2	79.6	4.0	0.11	–	–	–	–
N-TiO_2	60.4	3.8	0.09	–	–	0.33	0.21
N-TiO_2/AC	559	3.8	0.19	ca. 30%	ca. 58%	0.67	0.58

(–) Not applicable.
[a] Determined via gravimetry (ashing method).
[b] Determined via EDX analysis.
[c] Determined via XPS.

The characteristic of adsorption–desorption phenomenon as shown in Fig. 2 indicates that N-TiO_2/AC composite was a porous material. The inset shows that the predominant pore size of N-TiO_2/AC was ca. 3.8 nm, suggesting that this composite was mainly mesoporous.

XPS spectra (Fig. 3) reveal that the N1s peaks for N-TiO_2 and N-TiO_2/AC occurred at binding energy of ca. 399.7 eV and 400.8 eV, respectively. This indicates the formation of molecularly chemisorbed γ-N_2 onto the TiO_2 surface (binding energy of 400 eV and 402 eV) [13,26]. In other words, it also means that nitrogen atoms were interstitially doped into the TiO_2 crystal lattices [27]. The higher at% and mass% of surficial nitrogen in the N-TiO_2/AC composite (Table 1) as compared to that of N-TiO_2 might be due to the fact that supporting AC adsorbed some of the liberated ammonia during the decomposition of urea, hence resulted in additional incidental nitrogen doping for the composite. When both P25 and TiO_2 were used a reference, XPS verified that there was no detectable N1s peak on these photocatalysts.

The red-shift phenomenon exhibited by the as-synthesized N-TiO_2 in the visible-light region (ca. 400–550 nm region) was shown in the UV–vis absorbance spectra (Fig. 4). The estimated second absorbance edge for N-TiO_2 was ca. 2.25 eV (corresponding to light absorbance up to ca. 550 nm). The fact that TiO_2 did not exhibit significant absorbance in the visible-light spectrum as compared to N-TiO_2, indicated that it was urea (and not other foreign contaminants) which had contributed to the visible-light photoactivity effect of the N-TiO_2. This is in agreement with previous report [28] that nitrogen doping using urea resulted in the lowering of E_g of TiO_2 to ca. 2.3 eV, thus inducing desirable visible-light photoactivity properties. The UV–vis absorbance spectrum for N-TiO_2/AC was also analyzed (data not shown) and this black colour composite absorbs the whole spectrum of UV–vis light spectrum.

The anchorage of N-TiO_2 particles on the surface of AC is evidenced by TEM image (Fig. 5). The contrast in the features of N-TiO_2 crystals and the amorphous carbon could be observed. The insets (a and b) showed the selected area electron diffraction (SAED) pattern for the N-TiO_2 and AC, respectively. The presence of polycrystalline N-TiO_2 was indicated by the formation of concentric rings. AC did not exhibit this feature since it was predominantly amorphous. Given the non-uniform topology of AC surface, the thickness of the N-TiO_2 deposition was found to be varied. Nevertheless, N-TiO_2 coating of up to ca. 100 nm thickness was possible.

3.2. Adsorption studies

Fig. 6 depicts the adsorption isotherm of BPA on N-TiO_2/AC composite and virgin AC under the influence of solution pH. Langmuir adsorption isotherm model [29] was chosen for fitting the isotherm of BPA adsorption by N-TiO_2/AC and virgin AC. The corresponding adsorption parameters, such as maximum sorption capacity (S_{max}) and the adsorption constant (K_{ads}) are presented in Table 2. It was found that N-TiO_2/AC exhibited reductions in its adsorption capacity for BPA as compared to virgin AC for all

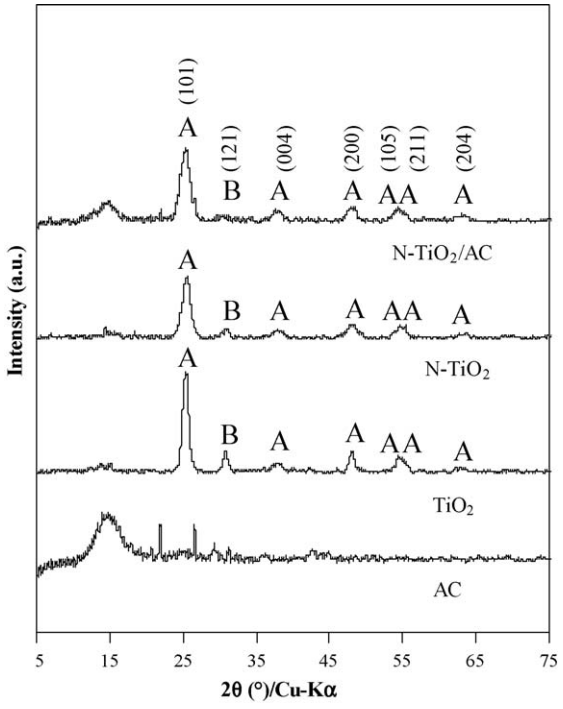

Fig. 1. XRD patterns for AC, TiO_2, N-TiO_2 and N-TiO_2/AC (*Note*: A and B denote anatase and brookite phases, respectively).

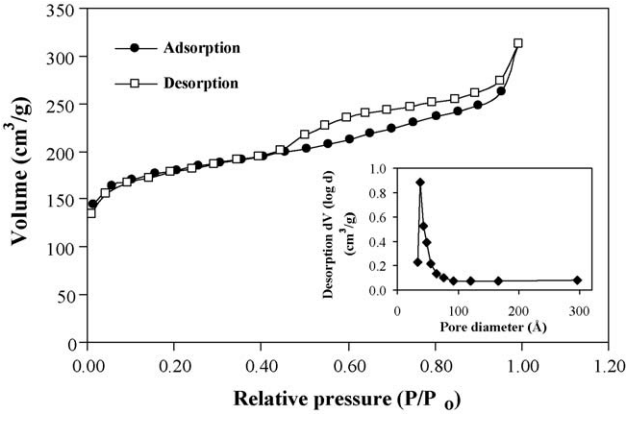

Fig. 2. Nitrogen adsorption–desorption isotherm analysis for N-TiO_2/AC (*Inset*: The corresponding pore size distribution for the composite).

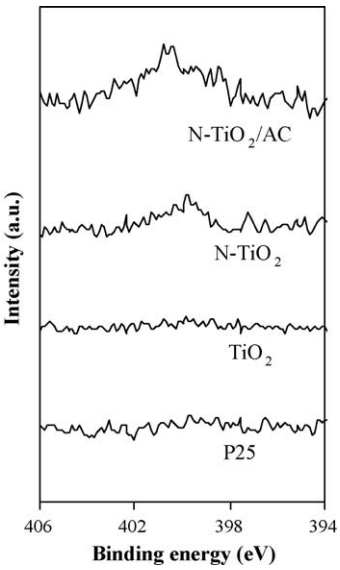

Fig. 3. XPS spectra depicting binding energy of N1s for N-TiO_2 and N-TiO_2/AC.

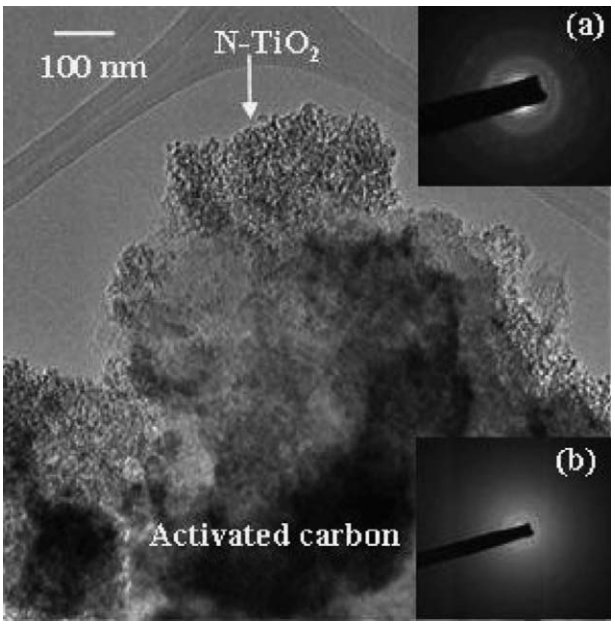

Fig. 5. TEM image depicting the anchorage of N-TiO2 on the surface of AC (*Inset*: (a) SAED pattern for N-TiO_2 crystals and (b) SAED pattern for AC).

investigated values of pH. This is due to the fact that N-TiO_2/AC possessed considerably lower S_{BET} than virgin AC.

Solution pH is an important environmental parameter as it governs the protonation/deprotonation of target compounds in the aqueous phase and the surface functional groups of AC, thus affecting the efficiency of adsorption and PCD. BPA adsorption on N-TiO_2/AC was found to be considerably inhibited at pH 11.0. BPA can deprotonate and formed monoanion ($HBPA^-$) and dianion (BPA^{2-}) at its pK_{a1} (9.59) and pK_{a2} (10.2), respectively [30]. Under alkaline condition, the AC surface functional groups would be negatively charged (AC-O^-) [31]. It is known that the pH_{pzc} (point of zero charge) for the TiO_2 is in the range of pH 5–7 [1,32]; i.e. a net positive and negative charge occurs on TiO_2 surface when $pH < pH_{pzc}$ and $pH > pH_{pzc}$, respectively. For the case of N-TiO_2, the pH_{pzc} has been reported to shift to a slightly higher value (ca. 1.0 unit pH only) as compared to the case of TiO_2 [14]. It is therefore postulated that BPA anions are considerably repelled by the predominant negatively charged functional groups present on the surface of N-TiO_2/AC at pH 11.0. In contrast, a relatively greater adsorption of BPA was exhibited by the composite at pH 3.0. Under acidic condition, positively charged surface functional groups formed on both AC (AC-OH_2^+) [31] and N-TiO_2 (≡Ti-OH_2^+) [1,32] will tend to have less electrostatic repulsion with the molecular form of BPA.

3.3. PCD studies

3.3.1. Effect of solution pH

At the end of 3 h of PCD experiment, the efficiency of PCD was found to generally decrease with increasing levels of pH (Fig. 7). The least BPA photodegradation at pH 11.0 was ascribed to the net electrostatic repulsion. Nevertheless, PCD of BPA at $pH > pK_{a2}$ still occurred because of the increasing OH^- ion concentrations in the solution. Reaction of OH^- with the photogenerated holes would produce hydroxyl radicals ($^{\bullet}OH$) to photocatalytically degrade BPA. The relatively improved BPA photodegradation in the acidic regime may be attributed to the positively charged surface groups on TiO_2 (≡Ti-OH_2^+) [1,32]. It has been reported that surface protonation of

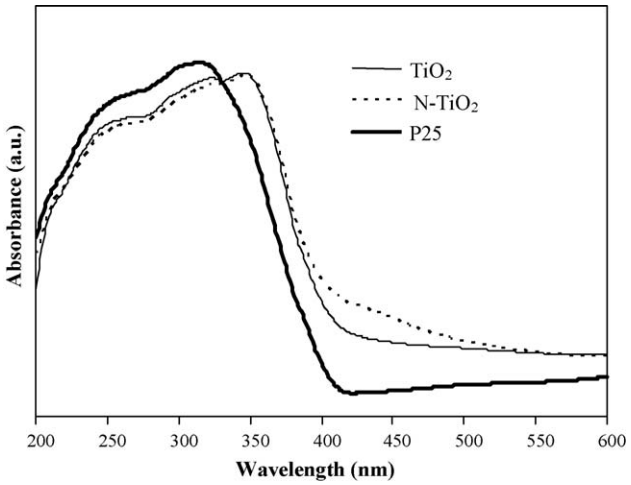

Fig. 4. UV–vis absorbance spectra for P25 and as-synthesized titania.

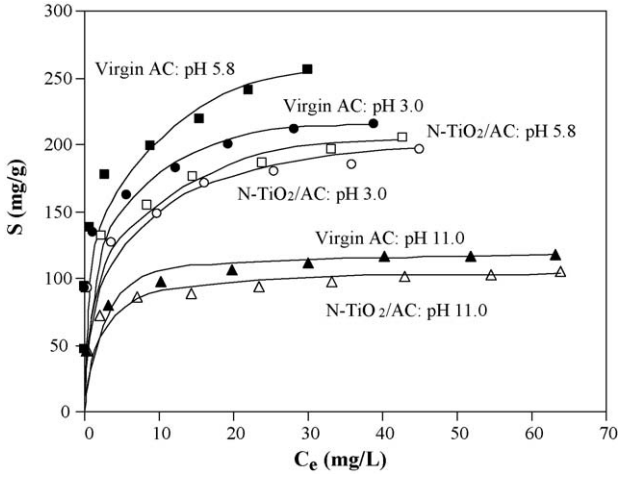

Fig. 6. Adsorption isotherm of BPA on virgin AC and N-TiO2/AC at different pH levels (*Note*: Symbols ○, ●, □, ■, △, ▲ denote experimental data; continuous curves are best-fitted based on Langmuir isotherm model).

Table 2
Adsorption parameters derived from the best-fitted Langmuir isotherm model.

Samples	pH	S_{max} (mg/g)	K_{ads} (L/mg)	R^2
Virgin AC	3.0 ± 0.2	217	1.05	0.996
	5.8 ± 0.2	252	1.13	0.992
	11.0 ± 0.2	120	0.58	0.999
N-TiO_2/AC	3.0 ± 0.2	196	0.62	0.995
	5.8 ± 0.2	204	0.74	0.995
	11.0 ± 0.2	106	0.54	0.998

TiO_2 in acidic solutions could lead to the production of photocurrent [33]. Thus, charge carriers separation could be relatively more favourable at acidic pH than at circumneutral and alkaline pH. Since our experiments did not involve aeration, thus it may be possible that the protonated surfaces of N-TiO_2 had compensated the role of dissolved oxygen as electron scavengers in the photocatalytic reaction system.

3.3.2. Effect of excitation wavelengths

The influence of excitation wavelengths on the photodegradation of BPA employing N-TiO_2/AC is presented in Fig. 8(a). After 3 h of solar irradiation, the blank experiment resulted in less than 4% of BPA removal through photolysis effect. It is postulated that the effect of photolysis would be further reduced in the presence of N-TiO_2/AC particles because of the significant light attenuation in the turbid solution. N-TiO_2/AC composite was found to be photoactive under both UV and visible-light illumination. Apparently, interstitial nitrogen doping for TiO_2 could result in desirable PCD effect. This demonstration of visible-light photoresponsiveness of N-TiO_2/AC is particularly encouraging as it indicates the potential of harnessing the visible-light energy from the solar irradiation, and possibly too, interior lightings. Given that nitrogen doping may result in visible-light absorbance up until ca. 550 nm (Fig. 4), further red-shift for the second absorbance edge onset may significantly improve PCD performance under visible-light irradiation. Further optimization of several pertinent factors such as crystallinity, porosity, nitrogen content (at%) in titania, loading of N-TiO_2 (wt%) in N-TiO_2/AC composite, and particle size of AC will also likely to improve PCD efficiency under visible-light.

The comparison of PCD efficiency achieved by N-TiO_2/AC with that of other photocatalysts is presented in Fig. 8(b). It was found that N-TiO_2/AC had relatively higher photodegradation efficiency for BPA after 3 h of experiment as compared with TiO_2, N-TiO_2 and P25. For the case of P25, its favourable PCD effect for solar and UV (280–400 nm) could partly be due to the presence of predominantly anatase–rutile mixture. However, in the visible-light range (420–630 nm), P25 displayed negligible removal of BPA. N-TiO_2 consistently exhibited greater BPA photodegradation efficiency than TiO_2 for all ranges of the investigated excitation wavelengths. In particular, N-TiO_2 exhibited more than two-fold PCD efficiency as compared to TiO_2 under visible-light illumination. This result is in agreement with the UV–vis absorbance results (Fig. 4). Indeed, synergistic effect of adsorption–photocatalysis exhibited by the dual-functional N-TiO_2/AC had resulted in greater BPA photodegradation, which otherwise was not achieved by the photocatalysts without AC support.

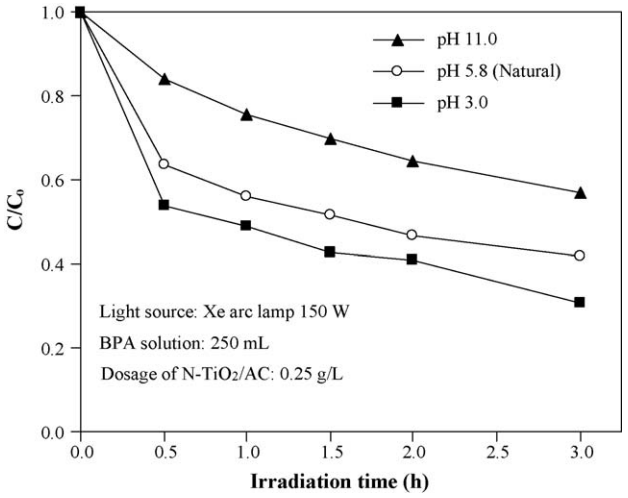

Fig. 7. Effect of pH on the photocatalytic degradation efficiency for BPA under simulated solar irradiation (*Note*: C_o denotes the equilibrium concentration of BPA after adsorption in the dark).

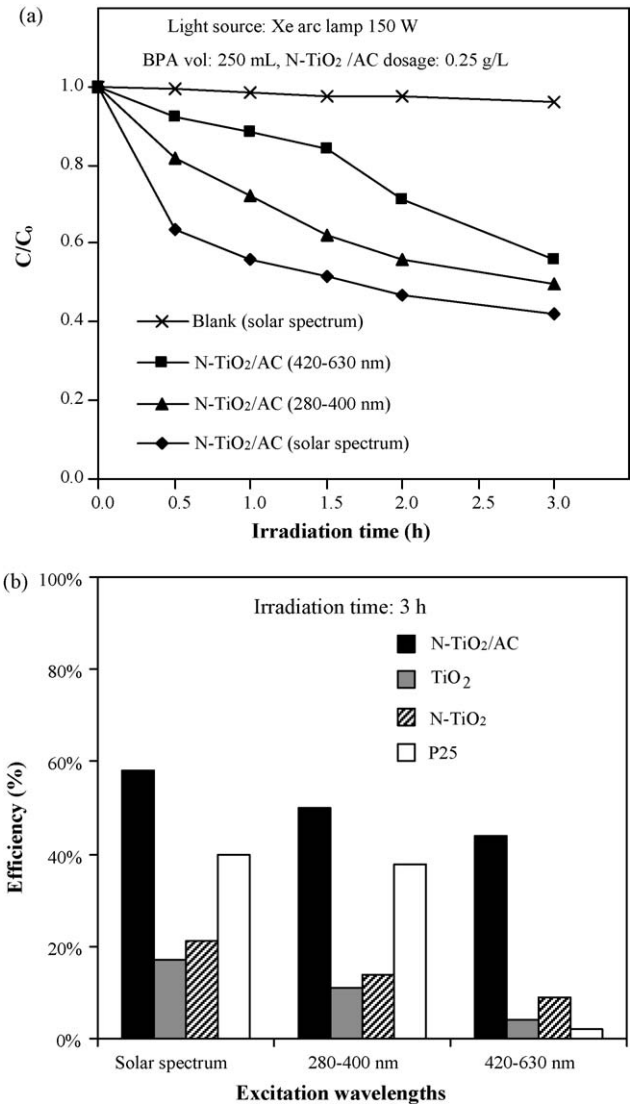

Fig. 8. (a) Effect of excitation wavelengths on the photocatalytic degradation efficiency for BPA (*Note*: C_o denotes the equilibrium concentration of BPA after adsorption in the dark) and (b) comparison of BPA removal performance under various excitation wavelengths for N-TiO_2/AC, TiO_2, N-TiO_2 and P25.

4. Conclusions and future work

A dual-functional composite, namely N-TiO_2/AC, which exhibited both adsorption and PCD effect, was synthesized using the sol–gel method and characterized. Interstitial nitrogen doping was verified with XPS analysis and the TEM image revealed the anchorage of N-TiO_2 on the surface of AC. PCD performance for BPA

was least at highly alkaline pH. The N-TiO_2/AC was photoactive under the irradiation of solar spectrum, UV (280–400 nm) and visible-light (420–630 nm). Future work shall address some of the aforementioned issues and to explore improved methods of synthesis for N-TiO_2/AC composite in order to yield greater removal efficiency for a wide range of recalcitrant aqueous organic contaminants with diverse molecular characteristics.

Acknowledgements

The research group acknowledges the financial support provided by the National Research Foundation (NRF), Singapore through project EWI RFP 0802-11. Pow-Seng Yap is grateful to Nanyang Technological University (NTU) for the award of a PhD research scholarship. Jebsen & Jessen Chemicals (S) Pte Ltd. is thanked for the generous provision of the Degussa P25.

References

[1] M.R. Hoffmann, S.T. Martin, W. Choi, D.W. Bahnemann, Chem. Rev. 95 (1995) 69–96.
[2] G. Li Puma, A. Bono, D. Krishnaiah, J.G. Collin, J. Hazard. Mater. 157 (2008) 209–219.
[3] T. Cordero, C. Duchamp, J.-M. Chovelon, C. Ferronato, J. Matos, J. Photochem. Photobiol. A: Chem. 191 (2007) 122–131.
[4] H.-W. Chen, Y. Ku, Y.-L. Kuo, Water Res. 41 (2007) 2069–2078.
[5] B. Sun, A.V. Vorontsov, P.G. Smirniotis, Langmuir 19 (2003) 3151–3156.
[6] C.-G. Wu, C.-C. Chao, F.-T. Kuo, Catal. Today 97 (2004) 103–112.
[7] A.-W. Xu, Y. Gao, H.-Q. Liu, J. Catal. 207 (2002) 151–157.
[8] I.M. Arabatzis, T. Stergiopoulos, M.C. Bernard, D. Labou, S.G. Neophytides, P. Falaras, Appl. Catal. B: Environ. 42 (2003) 187–201.
[9] A. Zaleska, J.W. Sobczak, E. Grabowska, J. Hupka, Appl. Catal. B: Environ. 78 (2008) 92–100.
[10] T. Ohno, M. Akiyoshi, T. Umebayashi, K. Asai, T. Mitsui, M. Matsumura, Appl. Catal. A: Gen. 265 (2004) 115–121.
[11] K. Kobayakawa, Y. Murakami, Y. Sato, J. Photochem. Photobiol. A: Chem. 170 (2005) 177–179.
[12] W. Choi, A. Termin, M.R. Hoffmann, J. Phys. Chem. 98 (1994) 13669–13679.
[13] R. Asahi, T. Morikawa, T. Ohwaki, K. Aoki, Y. Taga, Science 293 (2001) 269–271.
[14] H. Choi, M.G. Antoniou, M. Pelaez, A.A. de la Cruz, J.A. Shoemaker, D.D. Dionysiou, Environ. Sci. Technol. 41 (2007) 7530–7535.
[15] C. Brede, P. Fjeldal, I. Skjevrak, H. Herikstad, Food Addit. Contam.: Part A: Chem. Anal. Contr. Expos. Risk Assess. 20 (2003) 684–689.
[16] C.A. Staples, P.B. Dorn, G.M. Klecka, S.T. Oblock, L.R. Harris, Chemosphere 36 (1998) 2149–2173.
[17] W.-T. Tsai, J. Environ. Sci. Health, Pt. C 24 (2006) 225–255.
[18] J.-H. Kang, D. Aasi, Y. Katayama, Crit. Rev. Toxicol. 37 (2007) 607–625.
[19] F.S. vom Saal, W.V. Welshons, Environ. Res. 100 (2006) 50–76.
[20] V.K. Sharma, G.A.K. Anquandah, R.A. Yngard, H. Kim, J. Fekete, K. Bouzek, A.K. Ray, D. Golovko, J. Environ. Sci. Health, Part A 44 (2009) 423–442.
[21] G.-G. Ying, R.S. Kookana, A. Kumar, M. Mortimer, Sci. Total Environ. 407 (2009) 5147–5155.
[22] P. Pothitou, D. Voutsa, Chemosphere 73 (2008) 1716–1723.
[23] C. Höhne, W. Püttmann, Environ. Sci. Pollut. Res. 15 (2008) 405–416.
[24] P. Debye, P. Scherrer, Physikalische Zeitschrift 18 (1917) 291–301.
[25] Y. Li, S. Zhang, Q. Yu, W. Yin, Appl. Surf. Sci. 253 (2007) 9254–9258.
[26] N.C. Saha, H.G. Tompkins, J. Appl. Phys. 72 (1992) 3072–3079.
[27] C. Di Valentin, E. Finazzi, G. Pacchioni, A. Selloni, S. Livraghi, M.C. Paganini, E. Giamello, Chem. Phys. 339 (2007) 44–56.
[28] A.I. Kontos, A.G. Kontos, Y.S. Raptis, P. Falaras, Phys. Stat. Sol. (RRL)—Rapid Res. Lett. 2 (2008) 83–85.
[29] I. Langmuir, J. Am. Chem. Soc. 38 (1916) 2221–2295.
[30] P.G. Kosky, J.M. Silva, E.A. Guggenheim, Ind. Eng. Chem. Res. 30 (2002) 462–467.
[31] S.-J. Park, Y.-S. Jang, J. Colloid Interface Sci. 249 (2002) 458–463.
[32] W. Choi, Catal. Surv. Asia 10 (2006) 16–28.
[33] D.F. Watson, A. Marton, A.M. Stux, G.J. Meyer, J. Phys. Chem. B 107 (2003) 10971–10973.